


Provenance and paleoclimatic implications of loess deposits in Shandong Province, eastern China

Yongda Wang^{a,b,c} , Shiling Yang^{a,b,c*}, Zhongli Ding^a

^aKey Laboratory of Cenozoic Geology and Environment, Institute of Geology and Geophysics, Chinese Academy of Sciences, Beijing 100029, China

^bCAS Center for Excellence in Life and Paleoenvironment, Beijing 100044, China

^cCollege of Earth and Planetary Sciences, University of Chinese Academy of Sciences, Beijing 100049, China

*Corresponding author at: Key Laboratory of Cenozoic Geology and Environment, Institute of Geology and Geophysics, Chinese Academy of Sciences, Beijing 100029, China. E-mail address: yangsl@mail.iggcas.ac.cn (S. Yang).

(RECEIVED May 10, 2020; ACCEPTED October 26, 2020)

Abstract

The loess deposits in Shandong Province in eastern China potentially provide valuable insights into past environmental changes. However, their precise provenance and paleoclimatic implications are unclear. We studied three loess sections located in the piedmont of the Central Shandong Mountains (PCSM) and in an offshore island in Bohai Gulf. Both the glacial loess and interglacial paleosol units are characterized by a coarse grain size, indicating a proximal sediment source. Using the “grain size–transport distance” model established for the Chinese Loess Plateau (CLP), the estimated source–sink distance is ~200–300 km for the PCSM loess and ~100–200 km for the coastal loess. This suggests that fluvial deposits of the Yellow River system in the North China Plain and sediments on the adjacent continental shelf are the major provenance for the Shandong loess. In contrast to the CLP, the Shandong loess does not show a consistent pattern of coarse grain size and low magnetic susceptibility values in glacial loess compared with interglacial paleosols, likely due to frequent changes in dust sources caused by diversions of the Yellow River and local hydroclimatic conditions. Nevertheless, the loess–paleosol alternations in the Shandong loess are a product of global glacial–interglacial cycles.

Keywords: Loess; Shandong Province; OSL dating; Grain size; Magnetic susceptibility; Provenance; Paleoclimate

INTRODUCTION

Shandong Province in eastern China is one of the major areas of loess accumulation outside the Chinese Loess Plateau (CLP) (Fig. 1a and b) (Liu, 1985). Stratigraphic and sedimentological research on the Shandong loess has continued since the 1890s (Skertchly, 1895; Zdansky, 1925; Pearson, 1928; Yang, 1936; Liu, 1965), and chronological and paleoclimatic studies, as well as provenance investigations, have become a research focus since the 1980s (Li and Zhao, 1981; Cao et al., 1987; Xu et al., 2015, 2018; Tian et al., 2019). However, the provenance of the Shandong loess is debated. Early research, based on modern dust storm observations, suggested that the fine particles in the coastal loess of Shandong Province were transported by the East Asian winter monsoon from the arid region in northwestern China, while the coarse particles were derived from the adjacent continental shelf exposed

during glacial periods, transported by local northerly winds (Liu, 1985). Subsequently, the presence of marine microfossils (e.g., foraminifera and radiolarians) in the coastal loess suggested that the exposed continental shelf was an important source (Cao et al., 1987, 1993; Cheng et al., 1995, 1996; Zhao, 1996). For the loess deposits in the piedmont of the Central Shandong Mountains (PCSM) in Shandong Province, several researchers have proposed that they are a mixture of local dust from the adjacent floodplains or the continental shelf of Bohai Gulf and long-distance-transported dust from the arid region in northwestern China, on the basis of the characteristics of grain size, mineral and elemental composition, and the absence of marine microfossils (Zhang et al., 2004, 2005; Xin, 2005; Wang et al., 2014; Ding et al., 2015; Jia et al., 2016; Xu et al., 2016). However, other studies, using elemental analyses, have concluded that fluvial sediments in the North China Plain are the main source (Peng et al., 2016). Therefore, the provenance of the Shandong loess needs to be further investigated.

The loess deposits of the CLP are transported by the East Asian winter monsoon from the vast arid region in

Cite this article: Wang, Y., Yang, S., Ding, Z. 2021. Provenance and paleoclimatic implications of loess deposits in Shandong Province, eastern China. *Quaternary Research* 103, 88–98. <https://doi.org/10.1017/qua.2020.113>

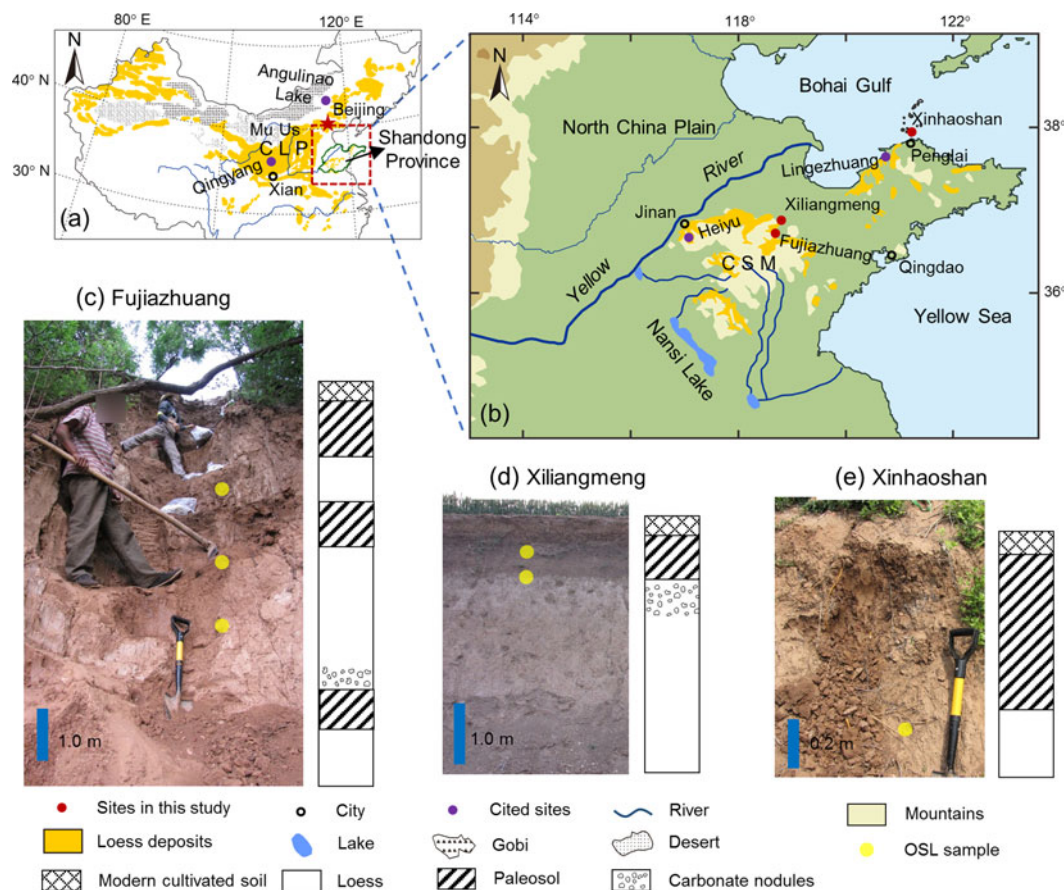


Figure 1. (color online) Distribution of loess deposits in China (a) (modified from Liu, 1985; Zhang et al., 2004); location of study sites (b) and photographs and stratigraphic columns of loess sections at Fujiazhuang (c), Xiliangmeng (d), and Xinhaoshan (e). CLP, Chinese Loess Plateau; CSM, Central Shandong Mountains. The locations of Lake Angulinao (Lu et al., 2018) and the loess sections at Heiyu (Kong, 2018), Lingezhuang (Tian et al., 2019), and Qingyang (Yang and Ding, 2008) are also shown.

northwestern China (e.g., Liu, 1985; Sun, 2002; Chen et al., 2007; Sun et al., 2008; Yan et al., 2014). Previous studies have demonstrated that the grain size of loess deposits in the CLP is controlled primarily by the source-to-sink distance: the greater the dust transport distance, the finer the grain size of the dust deposits (Yang and Ding, 2004, 2008, 2017; Ding et al., 2005). Thus, the grain size of the loess deposits in the CLP shows a southward-fining pattern, from which a model based on dust transport distance and grain-size parameters was developed (Yang and Ding, 2004, 2017). This approach can be used to explore the provenance of the Shandong loess.

In the CLP, the coarse grain size and low magnetic susceptibility (MS) values of the loess units indicate a cold and dry glacial climate, while the fine grain size and high MS of the paleosol units indicate a warm and humid interglacial climate (Heller and Liu, 1984; An et al., 1991; Ding et al., 1994, 2002; Yang and Ding, 2004, 2008, 2010). Therefore, grain size and MS have become two of the most widely used proxies for characterizing loess-paleosol stratigraphy. However, it remains unclear whether these two proxies are effective for characterizing loess-paleosol alternations (i.e., glacial-interglacial cycles) in loess deposits outside the CLP region.

Here we present grain size and MS records of three loess-paleosol sequences in Shandong Province. We then compare them with the results from previously studied loess sections in Shandong Province and the CLP, with the aim of addressing the provenance and paleoclimate significance of the Shandong loess.

GEOLOGICAL SETTING

The area of loess accumulation in Shandong Province lies within the warm temperate zone with a subhumid monsoon climate. The modern mean annual temperature and precipitation in the studied region are 11–14°C and 550–950 mm, respectively, with over 60% of the precipitation concentrated in the summer season. The landforms comprise mountains in the central part, plains in the west and north, and hills in the east (Bureau of Geology and Mineral Resources of Shandong Province, 1991). The loess deposits are distributed in the PCSM and the coastal area (including the offshore islands) of Bohai Gulf (Fig. 1b; Liu, 1985; Zhang et al., 2004). Typically they have thicknesses of <10 m (Zhang et al., 2004), and very thick (>30 m) loess sequences are preserved only in the PCSM (Zheng et al., 1994; Peng et al., 2011).

MATERIALS AND METHODS

Three loess sections—at Fujiazhuang (36°39.6'N, 118°26.8'E), Xiliangmeng (36°52.2'N, 118°28.5'E), and Xinhaoshan (37°54.8'N, 120°43.2'E) (Fig. 1b)—were logged and sampled. The Fujiazhuang and Xiliangmeng sections are situated in the PCSM and have elevations of ~163 m and ~23 m above sea level (asl), respectively. The Xinhaoshan section (~20 m asl) is situated in South Changshan Island near Penglai City (Fig. 1b).

Samples

In the Fujiazhuang section, the upper part (~7.45 m thick) was sampled. The section can be divided into seven stratigraphic units comprising a modern cultivated soil and three loess-paleosol couplets (Fig. 1c). The two paleosol layers (between the depths of 0.4 m and 3.05 m) in the upper part of the section are dark gray in color. Abundant carbonate nodules are present between the depths of 5.25 m and 5.65 m, immediately above the reddish paleosol unit in the lower part of the section. The Xiliangmeng section is 4 m thick and comprises three units from top to bottom: a modern cultivated soil, a darkish paleosol, and a yellowish loess unit (Fig. 1d). Below the paleosol unit (i.e., in the uppermost part of the loess unit), carbonate nodules are common between the depths of 1.05 m and 1.5 m. The Xinhaoshan section is 1.1 m thick, consisting of a modern cultivated soil, a brownish paleosol, and a yellowish loess, from top to bottom (Fig. 1e).

A total of 174 samples were taken at 5–10 cm intervals from the three sections for grain size and MS analyses. Six samples were also collected for optically stimulated luminescence (OSL) dating (Fig. 1c–e). In addition, a modern dust storm sample was collected in Penglai City (Fig. 1b), which is located ~13 km south of the Xinhaoshan section, to compare its grain-size characteristics with those of the samples from the loess sections.

Methods

Dating

Chinese loess is composed mainly of silt-sized particles (Liu, 1985; Yang and Ding, 2004, 2014; Peng et al., 2016; Xu et al., 2018) and thus is suitable for fine-grained quartz (4–11 µm) OSL dating (Aitken, 1985). This method has been widely used to date the loess deposits of the CLP (e.g., Lu et al., 2007; Kang et al., 2013), as well as those in Shandong Province (e.g., Peng et al., 2011; Kong et al., 2017; Li et al., 2019). In this study, the fine-grained quartz fraction (4–11 µm diameter) was selected for OSL dating. All samples were pre-treated with 30% H₂O₂ and 37% HCl to remove organic matter and carbonates, respectively. The 4–11 µm polymineralic fraction was separated according to Stokes' law and then immersed in 30% H₂SiF₆ for three days to obtain the fine-grained quartz component (Lu et al., 1988). Quartz aliquots

were deposited on 9.7-mm-diameter stainless steel discs using acetone for further experiments (Lu et al., 2007).

Optical luminescence measurements were made with an automated Daybreak 2200 OSL reader equipped with infrared (880 ± 60 nm) and blue (470 ± 5 nm) LED units and a ⁹⁰Sr/⁹⁰Y beta source (0.048 Gy/s) for irradiation (Lu et al., 2007). The stimulation conditions were 125°C for 50 s with a power of ~45 mW/cm² (Wang et al., 2005; Lu et al., 2007). Equivalent doses (D_e) were determined using the sensitivity-corrected multiple aliquot regenerative-dose (SMAR) protocol (Wang et al., 2005; Lu et al., 2007). These measurements were performed in the State Key Laboratory of Loess and Quaternary Geology in Xian. For dose rate determination, the concentrations of U (ppm), Th (ppm), and K (%) were measured using plasma emission spectrometry (U, Th) and inductively coupled plasma mass spectrometry (K) in the China Institute of Atomic Energy. The ages were calculated using the DRc program (Tsakalos et al., 2016) based on D_e and the dose rate.

MS and grain-size analyses

MS and grain-size analyses were conducted on bulk samples in the Key Laboratory of Cenozoic Geology and Environment, Chinese Academy of Sciences. Air-dried samples were weighed and packed in nonmagnetic plastic boxes and measured using a Bartington Instruments MS3 magnetic susceptibility meter. For grain-size analysis, samples of ~0.1–0.2 g were treated with diluted H₂O₂ and HCl on a hot plate to remove organic matter and carbonate, respectively. Ultrasonic treatment with the addition of a 0.05 mol/L solution of (NaPO₃)₆ was then used to disperse the samples before grain-size measurements, which were made using a Mastersizer 3000 laser particle-size analyzer.

RESULTS

Chronology

The OSL signals of all aliquots of each sample decayed to the background level in less than 10 seconds (Fig. 2a and d). The dose–response curve shows a growth trend denoting unsaturated signals (Fig. 2b and e). For each sample, the D_e values of all aliquots are normally distributed, suggesting that the quartz grains were bleached before burial (Fig. 2c and f). The average D_e of all aliquots was then used to calculate the age of the samples (Table 1).

The loess-paleosol units in the three sections are labeled using the L_i-S_j system, which is applied to the loess deposits of the CLP (Liu, 1985; Ding et al., 1993; Yang and Ding, 2010). The studied part of the Fujiazhuang section contains three paleosol units. The OSL samples from around the two closely spaced paleosols (0.4–3.05 m depth) in the upper part produced reversed dates: 11.0 ± 0.8 ka for the depth of 2.15 m and 8.5 ± 0.7 ka for the depth of 3.20 m (Fig. 3). The latter is around the transition from the glacial loess to the interglacial paleosol unit, which was possibly disturbed

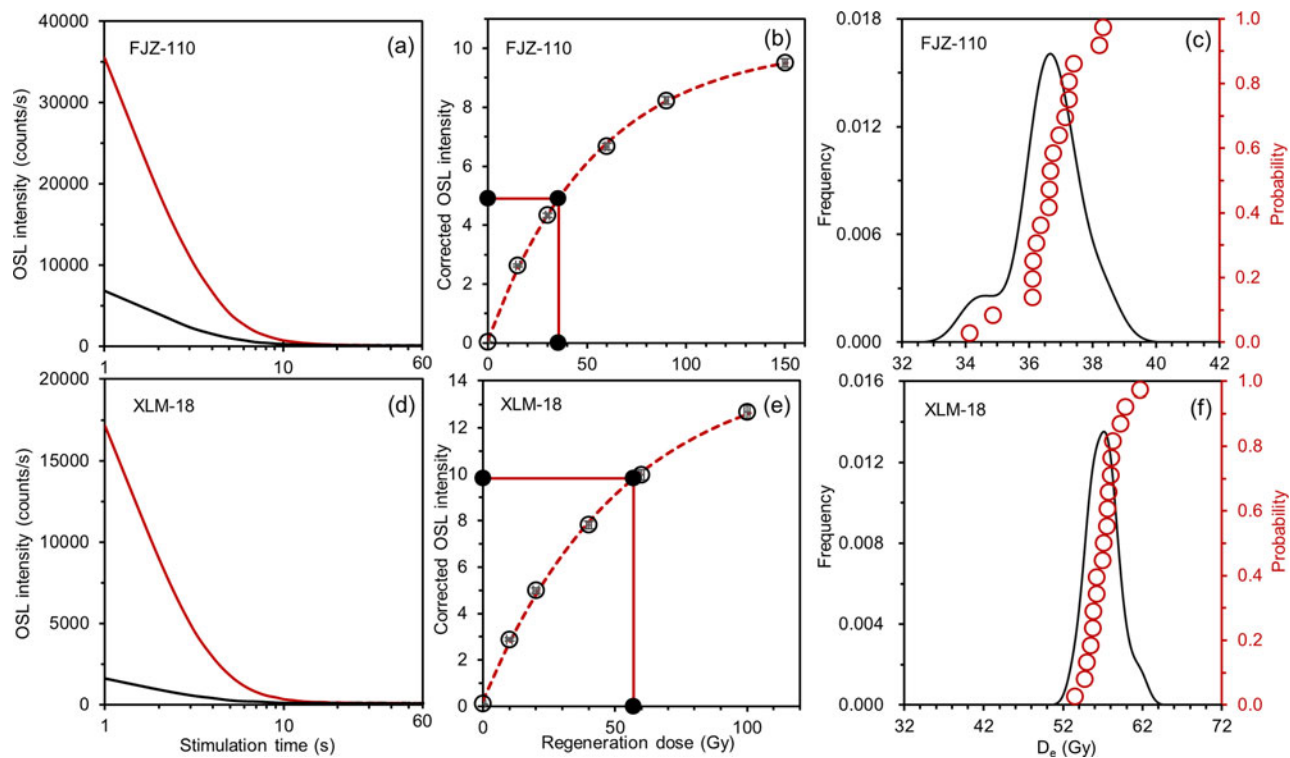


Figure 2. (color online) D_e determination for two representative samples from the Fujiiazhuang (FJZ-110; a–c) and Xiliangmeng (XLM-18; d–f) sections using the sensitivity-corrected multiple aliquot regenerative-dose (SMAR) protocol. (a, d) Decay curves of optically stimulated luminescence (OSL) intensity. (b, e) Corrected OSL dose response curves and D_e determination. (c, f) D_e distribution curves and cumulative probability curves.

by increased biological activity during interglacial soil development. This bioturbation can result in an OSL age that is younger than the sample’s burial age, which has been previously observed in eolian deposits (Bateman et al., 2007; Miao et al., 2010; Hanson et al., 2015). Despite the apparent age inconsistency, the results confirm that the two paleosols were developed during the Holocene; thus, they are designated S_{0-1} and S_{0-2} . The loess unit (L_1) below the Holocene soil unit (S_0) accumulated during the last glacial period, as indicated by the OSL age of 25.4 ± 4.0 ka at the depth of 4.3 m. The paleosol unit (S_1) in the lower part of the Fujiiazhuang section formed during the last interglacial period, according to previous studies (Fig. 3; Liu et al., 2000; Peng et al., 2011). The studied part of the Fujiiazhuang section is thus correlative with the loess-paleosol sequence of the last glacial–interglacial cycle in the CLP (Yang and Ding, 2014).

In the Xiliangmeng section, the paleosol unit underlying the modern cultivated soil is visually striking in the field because of its dark color. The OSL samples from the middle (0.65 m depth) and lower (0.9 m depth) parts of the paleosol have ages of 11.3 ± 1.0 ka and 18.5 ± 1.5 ka, respectively, indicating that this sequence was deposited mainly since the last glacial period (Fig. 3). Likewise, the Xinhaoshan loess deposits accumulated since the last glacial period, with a basal age of 12.0 ± 0.9 ka for the Holocene soil unit (S_0) (Fig. 3).

Grain-size distributions

The grain-size range of the loess samples from the Fujiiazhuang, Xiliangmeng, and Xinhaoshan sections is 0.4–200 μm , and the distributions are bimodal (Fig. 4). In the Fujiiazhuang and Xiliangmeng sections, the principal mode is

Table 1. OSL dating results for six samples from the Fujiiazhuang (FJZ), Xiliangmeng (XLM) and Xinhaoshan (XHS) sections.

Sample name	Depth (m)	U (ppm)	Th (ppm)	K (%)	Water content (%)	Dose rate (Gy/kyr)	D_e (Gy)	Age (ka)
FJZ-110	2.15	1.96 ± 0.20	10.98 ± 1.10	1.99 ± 0.20	19 ± 5	3.25 ± 0.23	35.89 ± 0.98	11.0 ± 0.8
FJZ-131	3.20	2.20 ± 0.22	13.10 ± 1.31	2.27 ± 0.23	20 ± 5	3.67 ± 0.26	31.36 ± 0.93	8.5 ± 0.7
FJZ-153	4.30	1.67 ± 0.17	9.66 ± 0.97	2.10 ± 0.21	21 ± 5	3.06 ± 0.21	77.59 ± 10.91	25.4 ± 4.0
XLM-13	0.65	2.59 ± 0.26	15.30 ± 1.53	2.06 ± 0.21	21 ± 5	3.79 ± 0.27	42.81 ± 2.25	11.3 ± 1.0
XLM-18	0.90	2.26 ± 0.23	11.17 ± 1.12	1.51 ± 0.15	15 ± 5	3.09 ± 0.22	57.10 ± 2.09	18.5 ± 1.5
XHS-20	1.05	1.91 ± 0.19	10.80 ± 1.08	1.98 ± 0.20	22 ± 5	3.14 ± 0.22	37.82 ± 0.90	12.0 ± 0.9

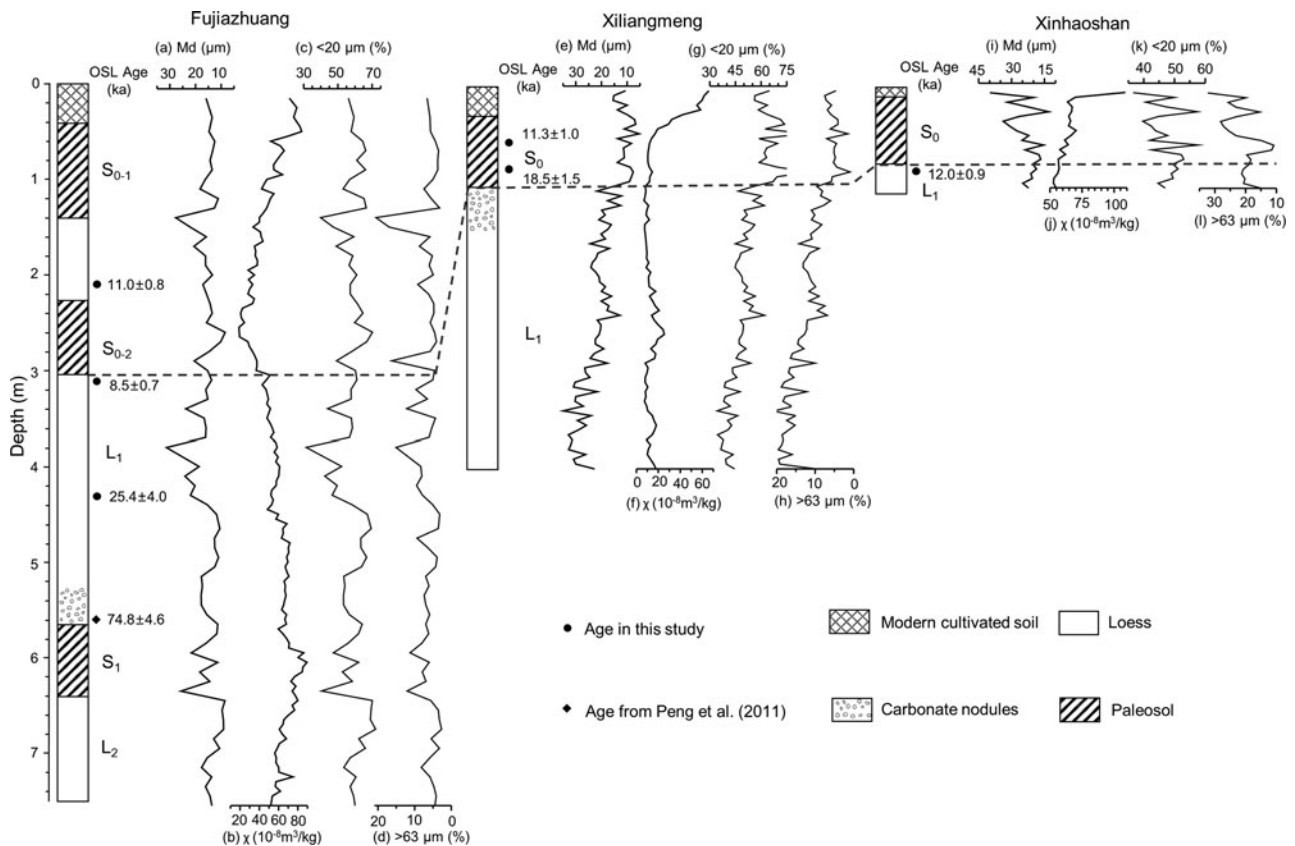


Figure 3. Optically stimulated luminescence (OSL) ages, median grain size (Md), magnetic susceptibility (χ), and grain size ($<20 \mu\text{m}\%$ and $>63 \mu\text{m}\%$) of the loess-paleosol sequences at Fujiiazhuang (a–d), Xiliangmeng (e–h), and Xinhaoshan (i–l).

between $30 \mu\text{m}$ and $40 \mu\text{m}$, and in the Xinhaoshan section it is between $30 \mu\text{m}$ and $70 \mu\text{m}$. In addition, all three sections have a secondary mode at $0.7\text{--}1 \mu\text{m}$ (Fig. 4a–c). The grain-size distributions of the paleosol samples are bimodal (e.g., the samples from the depths of 1.05 m [S_{0-1}] and 5.85 m [S_{1-1}], Fig. 4a), or trimodal (e.g., the samples from the depths of 2.65 m [S_{0-2}] and 5.95 m [S_{1-1}], Fig. 4a). The bimodal distribution is characterized by a principal mode at $30 \mu\text{m}$ or $50 \mu\text{m}$ and a minor mode at $<1 \mu\text{m}$, similar to the grain-size characteristics of the loess samples; by contrast, the trimodal distribution has two principal modes, of around $40 \mu\text{m}$ and $4 \mu\text{m}$ in the Fujiiazhuang and Xiliangmeng sections (Fig. 4a and b) and around 70 and $10 \mu\text{m}$ in the Xinhaoshan section (Fig. 4c). In addition, there is a minor mode at $<1 \mu\text{m}$ in all three sections (Fig. 4a–c). The modern dust sample from Penglai City has the grain-size range of $0.2\text{--}200 \mu\text{m}$; the distribution is bimodal with a principal mode at $60 \mu\text{m}$ and a secondary mode near $0.5 \mu\text{m}$ (Fig. 4d).

In contrast to the pattern of coarse loess grain size and fine paleosol grain size observed in loess-paleosol sequences across the CLP, the median grain size in the Fujiiazhuang section shows no systematic changes associated with the loess-paleosol alternations, except that several coarse grain-size spikes occur in both loess and paleosol units (Fig. 3a). Moreover, the S_1 paleosol unit is even coarser grained than the loess units above and below (Fig. 3a). In the Xiliangmeng section, the median grain-size values are centered around

$10 \mu\text{m}$ in S_0 and within the range of $15\text{--}35 \mu\text{m}$ in L_1 (Fig. 3e). In the Xinhaoshan section, S_0 has median grain sizes of 15 to $35 \mu\text{m}$ with large variations (Fig. 3i). The sand content ($>63 \mu\text{m}\%$) in the Fujiiazhuang and Xiliangmeng sections is generally less than 10% but reaches 20% in a few samples from soil units S_0 and S_1 , while the sand content is up to 30% in the Xinhaoshan section (Fig. 3). In all three sections, the sand content exhibits the same trend of variation as that of the median grain size, but the pattern is the opposite to that of the $<20 \mu\text{m}$ particle content (Fig. 3). In general, the grain size is finer in the loess deposits of the PCSM area (Fujiiazhuang and Xiliangmeng) than in those of the offshore island (Xinhaoshan).

Magnetic Susceptibility

In the three loess-paleosol sequences, both the loess and paleosol units are characterized by low MS values (Fig. 3). In the Fujiiazhuang section, the highest MS values ($\sim 80 \times 10^{-8} \text{ m}^3/\text{kg}$) are observed in the modern cultivated soil and in the last interglacial paleosol unit (S_1) (Fig. 3b), while the values for the Holocene soil (S_0) and the last glacial loess unit (L_1) fall within the range of $20\text{--}60 \times 10^{-8} \text{ m}^3/\text{kg}$ (Fig. 3b). In the Xiliangmeng section, the MS values are as low as $8\text{--}20 \times 10^{-8} \text{ m}^3/\text{kg}$, except for relatively high values in the modern cultivated soil (Fig. 3f). Likewise, in the Xinhaoshan section, the modern cultivated soil has high MS values ($>100 \times 10^{-8}$

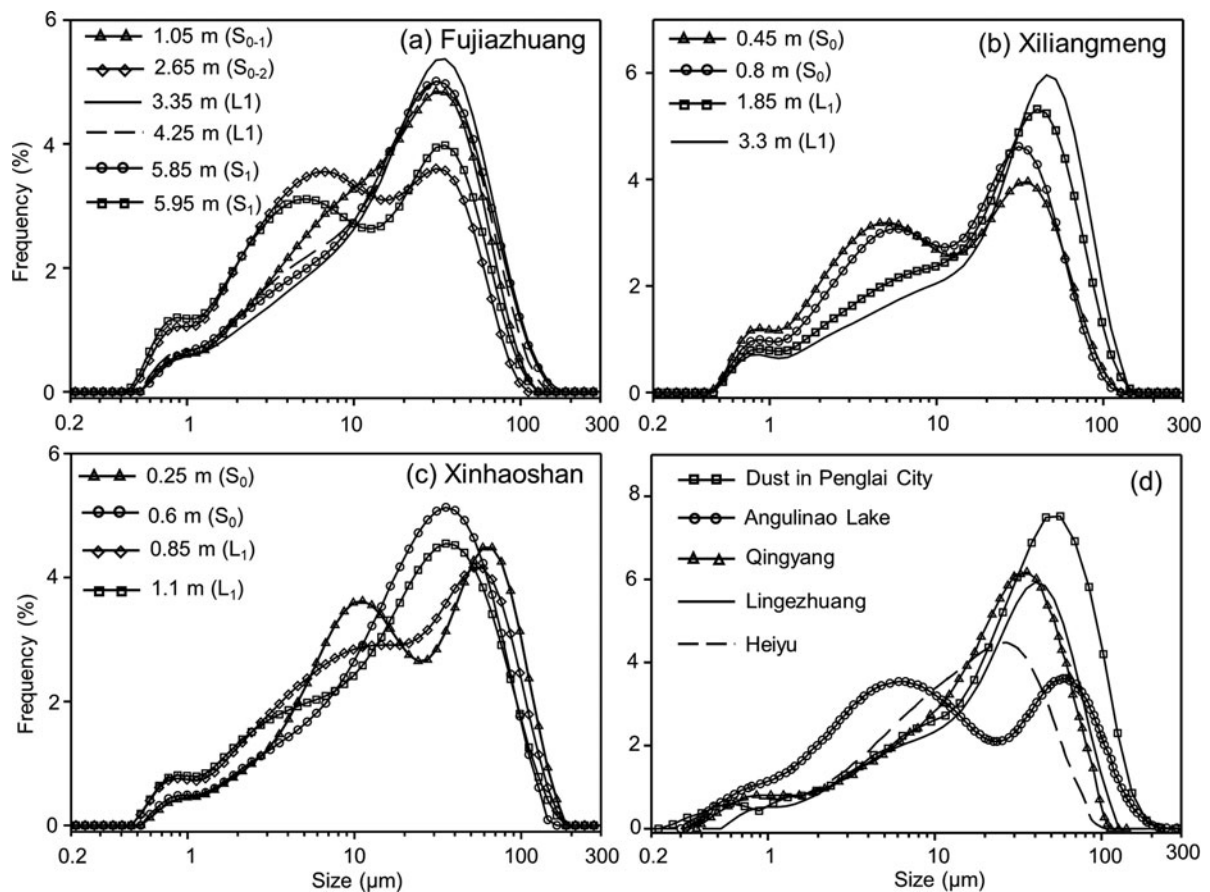


Figure 4. Grain-size distributions of representative samples from the Fujiiazhuang (a), Xiliangmeng (b), and Xinhaoshan (c) sections. Also shown are the grain-size distributions of a modern dust storm sample from Penglai City, loess samples from other sites in Shandong Province (Lingezhuang [Tian et al., 2019] and Heiyu [Kong, 2018]), the central Chinese Loess Plateau (Qingyang [Yang and Ding, 2008]), and a shallow lacustrine sample from Lake Angulinao in northeastern China (Lu et al., 2018) (d).

m^3/kg), whereas the underlying S_0 – L_1 couplet has low values ($\sim 60 \times 10^{-8} \text{ m}^3/\text{kg}$) (Fig. 3j).

DISCUSSION

Provenance of the Shandong loess

It is widely accepted that the arid region in northwestern China is the main source of the loess deposits of the CLP (e.g., Liu, 1985; Sun, 2002; Chen et al., 2007; Sun et al., 2008; Yan et al., 2014). Previous studies have shown that the grain size of loess is controlled primarily by the distance between the source area and the site of deposition, while the effect of the transporting wind intensity is minor (Ding et al., 1999, 2005; Yang and Ding, 2004, 2008, 2017). On the basis of the grain-size results for 53 loess sections from across the CLP, Yang and Ding (2008) found that with increasing distance to the southern margin of the Mu Us Desert, the median grain size of the last glacial loess unit (L_1) decreases rapidly from 50–60 μm in the north (within ~ 100 km of the desert margin) to 15–20 μm in the south (~ 360 km from the desert margin). For the last interglacial paleosol unit (S_1), the median grain size gradually decreases southward, from 14–16 μm

in the north to 8–9 μm in the south (Yang and Ding, 2004, 2008, 2017). On the basis of the spatial pattern of loess grain-size changes in the CLP, a relationship between grain size and dust transport distance was established (Yang and Ding, 2004, 2017):

$$\ln(Y) = -0.9231 \times \ln(X) + 8.108 \quad (R^2 = 0.986),$$

where X is the median grain size (μm) of loess deposits and Y (km) is the minimum source-to-sink distance.

The grain-size distributions of all of the loess samples and most of the paleosol samples in the Fujiiazhuang, Xiliangmeng, and Xinhaoshan sections are bimodal and positively skewed (Fig. 4). These characteristics are consistent with those of the modern dust (Fig. 4d) and of loess deposits in the CLP (Yang and Ding, 2004; Fig. 4d), indicating a typical aeolian origin of the Shandong loess. The last glacial loess unit L_1 in the three sections has a median grain-size range of 12–35 μm (Fig. 3), which is coarser than that of the L_1 loess unit in the southern part of the CLP (15–20 μm) but is similar to the contemporaneous loess unit in the central CLP (20–30 μm) (Yang and Ding, 2004). For the interglacial paleosols S_0 and S_1 , the median grain size has the range of 6–

35 μm (Fig. 3), which is also coarser than the contemporaneous paleosol unit in the southern part of the CLP (8–9 μm) (Yang and Ding, 2004). In addition, for the three loess sections in Shandong Province, there is no striking difference between the grain size of glacial loess and that of interglacial paleosol units, which contrasts with the pattern of “coarse-grained loess and fine-grained paleosol” commonly observed in the CLP (e.g., Yang and Ding, 2004, 2014).

Using the aforementioned “grain size–distance” model (Yang and Ding, 2004, 2017), we obtained a source–sink distance of ~200–300 km for the loess deposits in the PCSM and a distance of ~100–200 km for the loess deposits in the coastal area of Bohai Gulf. The estimated source–sink distances for the Shandong loess are much shorter than the distance to the arid region in northwestern China (>900 km) (Fig. 1); this indicates the importance of proximal, local dust sources for the Shandong loess, irrespective of glacial–interglacial cyclicality. Modern meteorological observations (Fu et al., 1994; Gao et al., 2008) and historical documents (Cai, 1989) have shown that dust activity in Shandong Province occurs mainly in spring when northeasterly winds prevail (Fig. 5), supporting a northeasterly provenance for the Shandong loess. Therefore, we conclude that the extensive fluvial deposits in the North China Plain and the continental shelf of Bohai Gulf, transported by the Yellow River and its tributaries (Wu et al., 1996, 2000; Xu et al., 1996), are the major sources of the Shandong loess. Previous studies have shown that elemental ratios ($\text{TiO}_2/\text{Al}_2\text{O}_3$, $\text{K}_2\text{O}/\text{Al}_2\text{O}_3$, and Na/K) (Peng et al., 2016; Xu et al., 2016, 2018), Nd–Sr isotope composition, and uranium isotope ratios ($^{234}\text{U}/^{238}\text{U}$) of the Shandong loess are strikingly different from those of the CLP loess, but comparatively close to those of sediments in lower reaches of the Yellow River (Li et al., 2017; Zheng, 2018). This evidence strongly supports our finding.

Comparison of the sections presented here with those in previous studies shows that the median grain size of both the glacial loess and interglacial paleosol units in the coastal area is coarser

than that of the corresponding units in the PCSM (Fig. 6). This indicates a substantial dust contribution from the adjacent continental shelf to the coastal loess, especially during the last glacial period when sea level fell substantially and desert steppe dominated the coastal areas (Fig. 6m–o; Liu and Xia, 1992; Liu et al., 2004; Yi et al., 2012; Li et al., 2014; Li et al., 2018), as supported by the presence of marine microfossils in the coastal loess (Cao et al., 1987, 1993; Cheng et al., 1995, 1996; Zhao, 1996). Furthermore, the prominent stratigraphic grain-size variability of the loess deposits of the PCSM indicates frequent changes in the location of dust sources due to frequent diversions of the Yellow River, which are documented in various historical records (e.g., Wu et al., 1996, 2000; Xu et al., 1996; Wang, 2005; Chen et al., 2012).

In addition, the trimodal grain-size distribution of a few paleosol samples from the Shandong loess (Fig. 4a–c) is similar to that of shallow lacustrine deposits in northeastern China (Lu et al., 2018; Fig. 4d), indicating the influence of enhanced hydrological conditions during interglacial periods. This is evidenced by the presence of gravels in a few loess sequences in Shandong Province (Zhang et al., 2004; Kong et al., 2019). Pollen records from alternating marine and fluvial sediments of the Bohai Gulf indicate the presence of broad-leaved forest–steppe vegetation in the North China Plain during the last interglacial period and Holocene, which coincided with a high sea level in Bohai Gulf and paleosol development in the Shandong loess areas (Fig. 6m–o; Liu et al., 2004; Yi et al., 2012; Li et al., 2018).

Paleoclimatic implications of the results

In the CLP, the grain size and MS of loess–paleosol sequences are reliable signals of the alternation of glacial loess and interglacial paleosol units (Heller and Liu, 1984; An et al., 1991; Ding et al., 1994, 2002; Yang and Ding, 2004, 2008, 2010); that is, the glacial loess units are characterized by a coarse grain size and low MS while the interglacial paleosol units

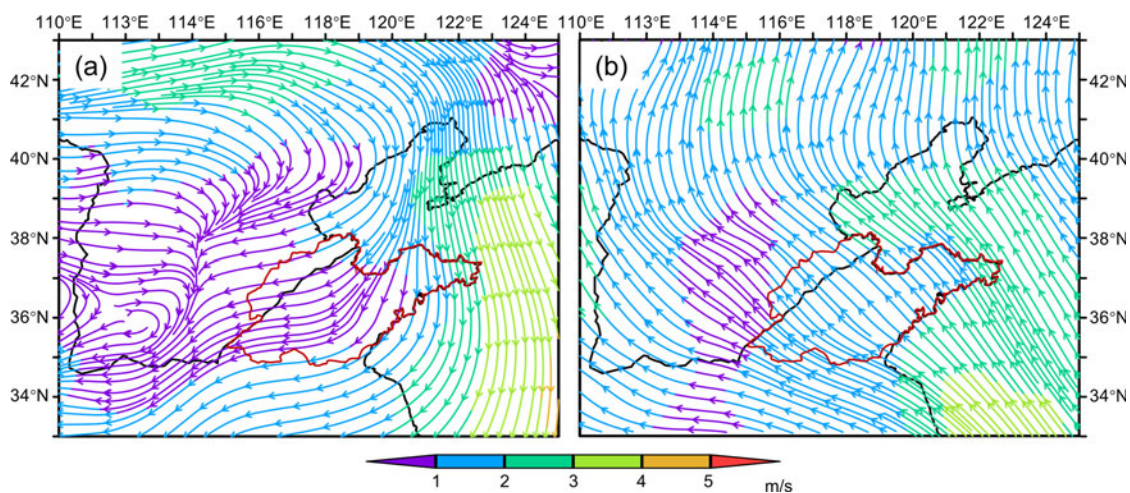


Figure 5. (color online) Surface circulation over Shandong Province. February–March mean surface winds (a) and July–August mean surface winds (b) based on the NOAA–CIRES–DOE Twentieth Century Reanalysis V3 data for January 1836 to December 2015 (https://psl.noaa.gov/data/gridded/data.20thC_ReanV3.html).

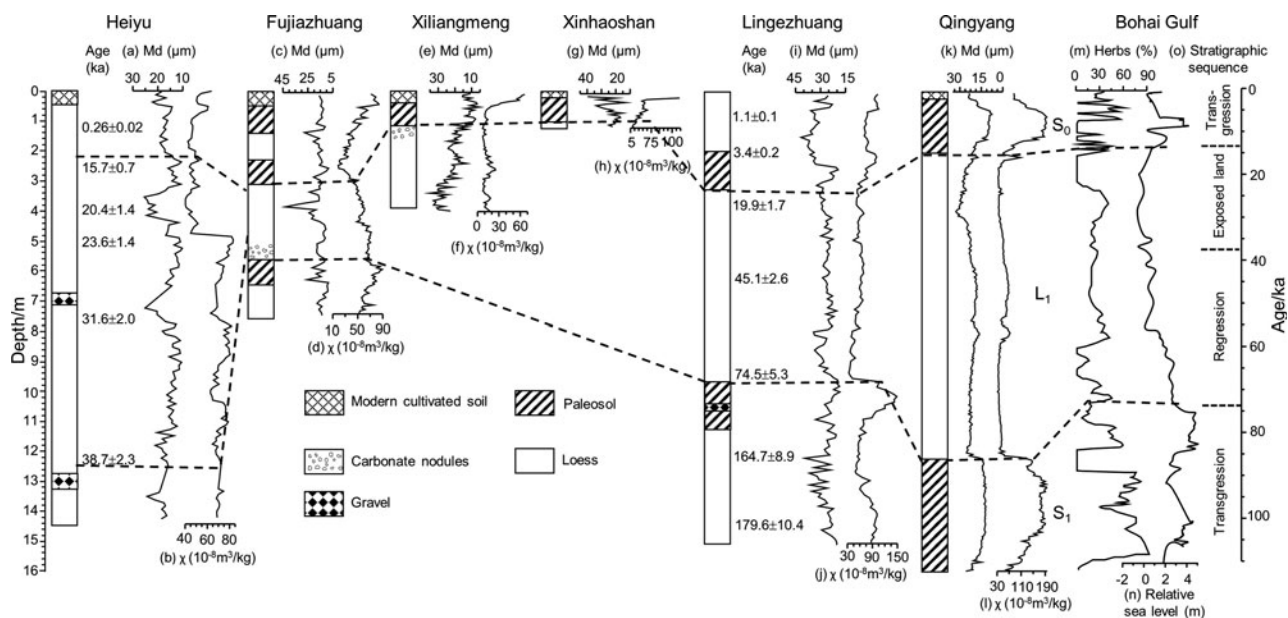


Figure 6. Comparison of the stratigraphy, median grain size (Md), and magnetic susceptibility (χ) records of loess sections in the piedmont of the Central Shandong Mountains (Heiyu [a, b], Fujiazhuang [c, d], and Xiliangmeng [e, f] [Kong, 2018]), the coastal area (Xinhaoshan [g, h] and Lingezhuang [i, j] [Tian et al., 2019]), and the central Chinese Loess Plateau (Qingyang [k, l] [Yang and Ding, 2008]). Pollen record (herb percentage; Li et al., 2018) and sea-level changes (Yi et al., 2012) in Bohai Gulf are also shown (m–o).

are characterized by a fine grain size and high MS. However, this pattern is not consistently observed in the Shandong loess. In contrast to the CLP, several parts of the Holocene soil unit (S_0) have almost the lowest MS values in both the Fujiazhuang and Xiliangmeng sections (Fig. 6). In addition, paleosol units S_1 in the Fujiazhuang section and S_0 in the Xinhaoshan section are coarser grained than the loess units above and below (Fig. 6). Therefore, the changes in grain size and MS in the Shandong loess do not effectively reflect loess-paleosol alternations.

The Shandong loess region lies to the east of the CLP and has a subhumid climate (Fig. 1b). Today, the climate is warmer and wetter in the Shandong loess region than in the CLP. The high organic matter content of the Holocene soil (S_0) at Fujiazhuang and Xiliangmeng, as indicated by its dark color, reflects a large vegetation biomass under a wet climate (Fig. 1c and d). Therefore, a gleying process due to a reducing soil environment may be responsible for the low MS values observed in paleosol S_0 unit. As mentioned in the preceding, the alternating loess and paleosol units during the last glacial–interglacial cycle in the Shandong loess region can be readily correlated with those in the CLP (Fig. 6; Yang and Ding, 2008; Kong, 2018; Tian et al., 2019). In this context, although the proxies for loess-paleosol stratigraphy developed in the CLP may not be applicable to the Shandong loess, the loess-paleosol alternations in both regions are a common product of global glacial–interglacial cycles.

CONCLUSIONS

OSL dating of the three loess sections in Shandong Province reveals that the Fujiazhuang loess-paleosol sequence

accumulated mainly since the last interglacial period and that the loess-paleosol sequences at Xiliangmeng and Xinhaoshan were deposited since the last glacial period.

The grain size of the glacial loess and interglacial paleosol units in Shandong Province is much coarser than that of the contemporaneous units in the southern part of the CLP but similar to those in the central CLP, indicating a proximal source for the Shandong loess. Using the grain size–transport distance model established for the CLP, the estimated source-sink distance is ~ 200 – 300 km for the loess deposits in the PCSM area and ~ 100 – 200 km for those in the coastal area. This suggests that the fluvial deposits of the Yellow River system in the North China Plain, as well as sediments on the adjacent continental shelf, are the major provenance for the Shandong loess. In the three studied sections, the grain-size distributions of most of the samples are bimodal and positively skewed; however, a trimodal distribution occurs in a few paleosol samples, indicating the effects of reworking by intensified hydrological processes on the Shandong loess during interglacial periods.

In contrast to the pattern of “coarse grain size and low MS of loess units” versus “fine grain size and high MS of paleosol units” observed in the loess-paleosol sequences of the CLP, several paleosol units in the Shandong loess are very coarse grained and have low MS values, probably due to frequent changes in dust sources caused by diversions of the Yellow River and local hydroclimatic conditions. Although the proxies for loess-paleosol stratigraphy developed in the CLP may not be applicable to the Shandong loess, the loess-paleosol alternations in the Shandong loess, like those of the CLP, are still a product of global glacial–interglacial cycles.

ACKNOWLEDGMENTS

This study was supported by the National Natural Science Foundation of China (grant 41725010), the Strategic Priority Research Program of Chinese Academy of Sciences (grants XDB31000000 and XDB26000000), and the Key Research Program of the Institute of Geology & Geophysics, CAS (grant IGGCAS-201905). We thank Yangyang Li and Xiaoxiao Yang for assistance in the field and laboratory. We are grateful to Nathaniel Rutter, Huayu Lu, and Nicholas Lancaster for their helpful comments and suggestions and Guest Editor Slobodan Marković for handling the manuscript.

REFERENCES

- Aitken, M.J., 1985. *Thermoluminescence Dating*. Academic Press, London.
- An, Z., Kukla, G.J., Porter, S.C., Xiao, J., 1991. Magnetic susceptibility evidence of monsoon variation on the loess plateau of central China during the last 130,000 years. *Quaternary Research* 36, 29–36.
- Bateman, M.D., Boulter, C.H., Carr, A.S., Frederick, C.D., Peter, D., Wilder, M., 2007. Preserving the palaeoenvironmental record in drylands: Bioturbation and its significance for luminescence-derived chronologies. *Sedimentary Geology* 195, 5–19.
- Bureau of Geology and Mineral Resources of Shandong Province, 1991. *Regional Geology of Shandong Province*. [In Chinese.] Geology Press, Beijing.
- Cai, G., 1989. The historical dust-fall documents in Shandong Province. [In Chinese.] *Journal of Catastrophology* 1, 59–63.
- Cao, J., Li, P., Shi, N., 1987. Loess of Miaodao islands in Shandong. [In Chinese.] *Science in China Series B* 17, 1116–1123.
- Cao, J., Liu, G., Shi, N., Chang, Y., Song, C., Yuan, H., Guo, X., 1993. Holocene loess of Miaodao islands in Shandong. [In Chinese with English abstract.] *Quaternary Sciences* 1, 25–33.
- Cheng, Z., Fu, M., Ju, X., 1996. Geological significance of paleontological fossils in coastal loess in the Bohai Strait and Liaodong Peninsula. [In Chinese with English abstract.] *Marine Geology & Quaternary Geology* 16, 85–94.
- Cheng, Z., Li, P., Lv, H., Ju, X., 1995. The radiolaria in the coastal loess in East Bohai Sea. [In Chinese with English abstract.] *Marine Sciences* 6, 59–64.
- Chen, J., Li, G., Yang, J., Rao, W., Lu, H., Balsam, W., Ji, J., 2007. Nd and Sr isotopic characteristics of Chinese deserts: Implications for the provenances of Asian dust. *Geochimica et Cosmochimica Acta* 71, 3904–3914.
- Chen, Y., Syvitski, J.P.M., Gao, S., Overeem, I., Kettner, A.J., 2012. Socio-economic impacts on flooding: A 4000-year history of the Yellow River, China. *Ambio: A Journal of the Human Environment* 41, 682–698.
- Ding, X., Cao, W., Xu, S., Ni, Z., 2015. Characteristics of rare earth elements in Pingyin loess profile, Shandong Province and its implications for provenance. [In Chinese with English abstract.] *Journal of Arid Land Resources and Environment* 29, 188–192.
- Ding, Z., Derbyshire, E., Yang, S., Sun, J., Liu, T., 2005. Stepwise expansion of desert environment across northern China in the past 3.5 Ma and implications for monsoon evolution. *Earth and Planetary Science Letters* 237, 45–55.
- Ding, Z., Derbyshire, E., Yang, S., Yu, Z., Xiong, S., Liu, T., 2002. Stacked 2.6-Ma grain size record from the Chinese loess based on five sections and correlation with the deep-sea $\delta^{18}\text{O}$ record. *Paleoceanography* 17, 5-1–5-21.
- Ding, Z., Rutter, N., Liu, T., 1993. Pedostratigraphy of Chinese loess deposits and climatic cycles in the last 2.5 Myr. *Catena* 20, 73–91.
- Ding, Z., Sun, J., Liu, D., 1999. A sedimentological proxy indicator linking changes in loess and deserts in the Quaternary. *Science in China Series D* 42, 146–152.
- Ding, Z., Yu, Z., Rutter, N., Liu, T., 1994. Towards an orbital time scale for Chinese loess deposits. *Quaternary Science Reviews* 13, 39–70.
- Fu, M., Xu, X.S., Cheng, Z., Xu, X.W., 1994. The seasonal desertification-climate environment in the coastal areas of the Yellow Sea and Bohai Sea. [In Chinese with English abstract.] *Journal of Desert Research* 14, 31–40.
- Gao, R., Wang, S., Zhang, X., Song, H., Gao, H., Zang, K., 2008. An analysis of the climatic characteristics of the gale in Bohai Straits. [In Chinese with English abstract.] *Marine Forecasts* 25, 7–15.
- Hanson, P.R., Mason, J.A., Jacobs, P.M., Young, A.R., 2015. Evidence for bioturbation of luminescence signals in eolian sand on upland ridgetops, southeastern Minnesota, USA. *Quaternary International* 362, 108–115.
- Heller, F., Liu, T., 1984. Magnetism of Chinese loess deposits. *Geophysical Journal of the Royal Astronomical Society* 77, 125–141.
- Jia, G., Xu, S., Kong, F., Ding, X., 2016. Characteristics and significance of rare earth elements in loess of Shandong region. [In Chinese with English abstract.] *Journal of Zaozhuang University* 33, 129–134.
- Kang, S., Wang, X., Lu, Y., 2013. Quartz OSL chronology and dust accumulation rate changes since the Last Glacial at Weinan on the southeastern Chinese Loess Plateau. *Boreas* 42, 815–829.
- Kong, F., 2018. *Fabric characteristics of gravel layer in the loess of the Zhangqiu, Shandong Province*. [In Chinese with English abstract.] Master's thesis, Shandong Normal University, Jinan.
- Kong, F., Xu, S., Jia, G., 2017. Climatic and environmental evolution with multi-index records of the loess in the Focun, Zibo, Shandong Province. [In Chinese with English abstract.] *Journal of Earth Environment* 8, 407–418.
- Kong, F., Xu, S., Jia, G., 2019. Research progress of gravel layer in Shandong Loess. [In Chinese with English abstract.] *Journal of Stratigraphy* 43, 81–88.
- Li, G., Li, L., Xu, S., Li, X., Chen, J., 2017. Dust source of the loess deposits in the eastern China constrained by uranium comminution age. [In Chinese with English abstract.] *Quaternary Sciences* 37, 1037–1044.
- Li, G., Li, P., Liu, Y., Qiao, L., Ma, Y., Xu, J., Yang, Z., 2014. Sedimentary system response to the global sea level change in the East China Seas since the last glacial maximum. *Earth Science Reviews* 139, 390–405.
- Li, J., Li, R., Yang, S., Chen, X., Chen, S., 2018. Pollen spore assemblages and induced palaeoenvironmental changes in the western Bohai Sea since Late Pleistocene. [In Chinese with English abstract.] *Marine Geology & Quaternary Geology* 38, 115–128.
- Liu, E., Zhang, Z., Shen, J., 2004. Spore-pollen records of environmental change on south coast plain of Laizhou Bay since the Late Pleistocene. [In Chinese with English abstract.] *Journal of Palaeogeography* 6, 78–84.
- Liu, L., Li, P., Wang, Y., 2000. The grain-size properties and genesis of the loess in central Shandong Province. [In Chinese with English abstract.] *Marine Geology & Quaternary Geology* 20, 81–86.
- Liu, T., 1965. *The Loess Deposits in China*. [In Chinese.] China Science Press, Beijing.

- Liu, T., 1985. *Loess and the Environment*. China Ocean Press, Beijing.
- Liu, Z., Xia, D., 1992. Sedimental characteristics of ancient desert in Bohai Sea. [In Chinese with English abstract.] *Acta Sedimentologica Sinica* 10, 94–99.
- Li, W., Li, Z., Wang, Z., Ma, Z., Wang, Z., Liang, L., 2019. Climatic environment changes during the last interglacial-glacial cycle in Zhifu loess section: Revealed by grain-size end-member algorithm. [In Chinese with English abstract.] *Marine Geology & Quaternary Geology* 39, 177–187.
- Li, W., Zhao, Q., 1981. Preliminary study of the Quaternary sediments in Miaodao Islands. [In Chinese with English abstract.] *Marine Sciences* 3, 20–22.
- Lu, Y., Fang, X., Friedrich, O., Song, C., 2018. Characteristic grain-size component: A useful process-related parameter for grain-size analysis of lacustrine clastics? *Quaternary International* 479, 90–99.
- Lu, Y., Wang, X., Wintle, A.G., 2007. A new OSL chronology for dust accumulation in the last 130,000 yr for the Chinese Loess Plateau. *Quaternary Research* 67, 152–160.
- Lu, Y., Zhang, J., Xie, J., 1988. Thermoluminescence dating of loess and paleosols from the Lantian section, Shaanxi Province, China. *Quaternary Science Reviews* 7, 245–250.
- Miao, X., Hanson, P.R., Wang, H., Young, A.R., 2010. Timing and origin for sand dunes in the Green River Lowland of Illinois, upper Mississippi River Valley, USA. *Quaternary Science Reviews* 29, 763–773.
- Pearson, H.S., 1928. Chinese fossil Suidae. *Palaeontologia Sinica* C 5, 1–75.
- Peng, S., Hao, Q., Wang, L., Ding, M., Zhang, W., Wang, Y., Guo, Z., 2016. Geochemical and grain-size evidence for the provenance of loess deposits in the Central Shandong Mountains region, northern China. *Quaternary Research* 85, 290–298.
- Peng, S., Zhu, L., Xiao, G., Qiao, Y., Gao, Z., Chen, D., 2011. Magnetostratigraphy and provenance of the Qingzhou loess in Shandong Province. *Journal of Arid Land* 3, 184–190.
- Skertchly, S.B.L., 1895. Concerning about loess and other deposits of North China. *The Quarterly Journal of the Geological Society of London* 51, 11–20.
- Sun, J., 2002. Provenance of loess material and formation of loess deposits on the Chinese Loess Plateau. *Earth and Planetary Science Letters* 203, 845–859.
- Sun, Y., Tada, R., Chen, J., Liu, Q., Toyoda, S., Tani, A., Ji, J., Isozaki, Y., 2008. Tracing the provenance of fine-grained dust deposited on the central Chinese Loess Plateau. *Geophysical Research Letters* 35, L01804.
- Tian, S., Sun, J., Lü, L., Cao, M., Zhang, Z., Lü, T., 2019. Optically stimulated luminescence dating of late Quaternary loess deposits in the coastal region of North China: Provenance and paleoclimatic implications. *Quaternary Science Reviews* 218, 160–177.
- Tsakalos, E., Christodoulakis, J., Charalambous, L., 2016. The dose rate calculator (DRc) for luminescence and ESR dating—A java application for dose rate and age determination. *Archaeometry* 58, 347–352.
- Wang, R., 2005. Northward removal channels of the Huanghe River and prehistoric disaster event: Discussion with Mr. Ren Mei -E. [In Chinese with English abstract.] *Scientia Geographica Sinica* 25, 294–298.
- Wang, X., Lu, Y., Li, X., 2005. Luminescence dating of fine-grained quartz in Chinese loess—Simplified Multiple Aliquot Regenerative-dose (MAR) protocol. [In Chinese with English abstract.] *Seismology and Geology* 27, 615–622.
- Wang, Y., Peng, S., Feng, Z., Zhang, W., Ding, M., 2014. Grain-size characteristics of loess deposits and its implication in the northern piedmont of the central Shandong mountainous region. [In Chinese with English abstract.] *Journal of Arid Land Resources and Environment* 28, 156–160.
- Wu, C., Xu, Q., Yang, X., 2000. Ancient drainage system of the Yellow River on North China Plain. [In Chinese with English abstract.] *Journal of Geomechanics* 6, 1–9.
- Wu, C., Xu, Q., Zhang, X., Ma, Y., 1996. Palaeochannels on the North China Plain: Types and distributions. *Geomorphology* 18, 5–14.
- Xin, L., 2005. Characteristics of the composition of the Zhangxia loess and its origin. [In Chinese with English abstract.] *Geology in China* 32, 55–61.
- Xu, Q., Wu, C., Zhu, X., Yang, X., 1996. Palaeochannels on the North China Plain: Stage division and palaeoenvironments. *Geomorphology* 18, 15–25.
- Xu, S., Ding, X., Yu, L., Ni, Z., 2015. Palaeoclimatic implications of aeolian sediments on the Miaodao Islands, Bohai Sea, East China, based on OSL dating and proxies. *Aeolian Research* 19, 259–266.
- Xu, S., Kong, F., Jia, G., Miao, X., Ding, X., 2018. An integrated OSL chronology, sedimentology and geochemical approach to loess deposits from Tuoji Island, Shandong Province: Implications for the late quaternary paleoenvironment in East China. *Aeolian Research* 31, 105–116.
- Xu, S., Ni, Z., Ding, X., 2016. Geochemical characteristics of major elements of the Pingyin loess in Shandong Province. [In Chinese with English abstract.] *Bulletin of Mineralogy, Petrology and Geochemistry* 35, 353–359.
- Yang, S., Ding, Z., 2004. Comparison of particle size characteristics of the Tertiary ‘red clay’ and Pleistocene loess in the Chinese Loess Plateau: Implications for origin and sources of the ‘red clay’. *Sedimentology* 51, 77–93.
- Yang, S., Ding, Z., 2008. Advance–retreat history of the East-Asian summer monsoon rainfall belt over northern China during the last two glacial–interglacial cycles. *Earth and Planetary Science Letters* 274, 499–510.
- Yang, S., Ding, Z., 2010. Drastic climatic shift at ~2.8 Ma as recorded in eolian deposits of China and its implications for redefining the Pliocene–Pleistocene boundary. *Quaternary International* 219, 37–44.
- Yang, S., Ding, Z., 2014. A 249 kyr stack of eight loess grain size records from northern China documenting millennial-scale climate variability. *Geochemistry, Geophysics, Geosystems* 15, 798–814.
- Yang, S., Ding, Z., 2017. Spatial changes in grain size of loess deposits in the Chinese Loess Plateau and implications for paleoenvironment. [In Chinese with English abstract.] *Quaternary Sciences* 37, 934–944.
- Yang, Z., 1936. On the Cenozoic geology of Itu, Changlo and Linchv, Shantung. *Bulletin of the Geological Society of China* 15, 171–187.
- Yan, Y., Sun, Y., Chen, H., Ma, L., 2014. Oxygen isotope signatures of quartz from major Asian dust sources: Implications for changes in the provenance of Chinese Loess. *Geochimica et Cosmochimica Acta* 139, 399–410.
- Yi, L., Yu, H., Ortiz, J.D., Xu, X., Qiang, X., Huang, H., Shi, X., Deng, C., 2012. A reconstruction of late Pleistocene relative sea level in the south Bohai Sea, China, based on sediment grain-size analysis. *Sedimentary Geology* 281, 88–100.
- Zdansky, O., 1925. Fossil Hirsche Chinas. *Palaeontologia Sinica* C 2, 1–94.

- Zhang, Z., Xin, L., Jiang, L., Jiang, L., Huang, P., 2005. Sedimentary characteristics and genetic analysis of Zhangxia Loess in Jinan, Shandong Province. [In Chinese with English abstract.] *Journal of Palaeogeography* 7, 98–106.
- Zhang, Z., Xin, L., Nie, X., 2004. A summary of loessial researches in Shandong. [In Chinese with English abstract.] *Scientia Geographica Sinica* 24, 746–752.
- Zhao, Q., 1996. Re-analysis of microfossils in Miaodao loess, Bohai Sea. [In Chinese.] *Science in China Series D* 26, 445–451.
- Zheng, H., Zhu, Z., Huang, B., Lu, L., 1994. A study on loess geochronology of Shandong Peninsula and northern part of Jiangsu and Anhui Provinces. [In Chinese with English abstract.] *Marine Geology & Quaternary Geology* 14, 63–68.
- Zheng, L., 2018. Provenances of the major loess deposits in eastern China based on Sr and Nd isotopic characteristics. [In Chinese with English abstract.] *Geological Journal of China Universities* 24, 246–250.